

Metadata of the chapter that will be visualized in SpringerLink

Book Title	Direct and Large-Eddy Simulation XI	
Series Title		
Chapter Title	Benchmark on the Aerodynamics of a 5:1 Rectangular Cylinder: Further Experimental and LES Results	
Copyright Year	2019	
Copyright HolderName	Springer Nature Switzerland AG	
Corresponding Author	Family Name	Mannini
	Particle	
	Given Name	C.
	Prefix	
	Suffix	
	Role	
	Division	Dip. Ingegneria Civile e Ambientale
	Organization	Università di Firenze
	Address	Via S. Marta 3, Firenze, 50139, Italia
	Email	claudio.mannini@unifi.it
Author	Family Name	Mariotti
	Particle	
	Given Name	A.
	Prefix	
	Suffix	
	Role	
	Division	Dip. Ingegneria Civile e Industriale
	Organization	Università di Pisa
	Address	Via G. Caruso 8, Pisa, 56122, Italia
	Email	alessandro.mariotti@for.unipi.it
Author	Family Name	Siconolfi
	Particle	
	Given Name	L.
	Prefix	
	Suffix	
	Role	
	Division	Dip. Ingegneria Civile e Industriale
	Organization	Università di Pisa
	Address	Via G. Caruso 8, Pisa, 56122, Italia
	Email	siconolfi.lorenzo@gmail.com
Author	Family Name	Salveti
	Particle	
	Given Name	M. V.
	Prefix	
	Suffix	

Role
Division Dip. Ingegneria Civile e Industriale
Organization Università di Pisa
Address Via G. Caruso 8, Pisa, 56122, Italia
Email mv.salvetti@ing.unipi.it

Abstract

The flow around a rectangular cylinder, having chord-to-depth ratio equal to 5, has been the object of a benchmark (BARC) launched in 2008 (<http://www.aniv-iawe.org/barc/>). The BARC configuration is of practical interest, e.g. in civil engineering, and, in spite of the simple geometry, the related flow dynamics and topology is complex. Indeed, the high-Reynolds-number flow around such a stationary rectangular cylinder is turbulent with flow separation from the upstream corners and unsteady reattachment on the cylinder side. Furthermore, a vortex shedding also occurs from the rear corners and interferes with the leading-edge vortices, according to the mechanism of impinging shear-layer instability (Nakamura et al, J Fluid Mech, 222:437–447, 1991, [1]).

Benchmark on the Aerodynamics of a 5:1 Rectangular Cylinder: Further Experimental and LES Results



C. Mannini, A. Mariotti, L. Siconolfi and M.V. Salvetti

1 Introduction

The flow around a rectangular cylinder, having chord-to-depth ratio equal to 5, has been the object of a benchmark (BARC) launched in 2008 (<http://www.aniv-iawe.org/barc/>). The BARC configuration is of practical interest, e.g. in civil engineering, and, in spite of the simple geometry, the related flow dynamics and topology is complex. Indeed, the high-Reynolds-number flow around such a stationary rectangular cylinder is turbulent with flow separation from the upstream corners and unsteady reattachment on the cylinder side. Furthermore, a vortex shedding also occurs from the rear corners and interferes with the leading-edge vortices, according to the mechanism of impinging shear-layer instability [1].

The experimental and numerical results obtained by the benchmark contributors during the first four years of activity were summarized and reviewed in [2]. Good agreement between different results in terms of near-wake flow, base pressure and drag coefficient was found. However, it was observed that some quantities of interest, as the standard deviation of the lift coefficient or the distribution of mean and fluctuating pressure on the cylinder sides, are affected by a significant dispersion, both in experiments and in simulations. Sensitivity analyses carried out by the BARC

C. Mannini (✉)

Dip. Ingegneria Civile e Ambientale, Università di Firenze,
Via S. Marta 3, Firenze 50139, Italia
e-mail: claudio.mannini@unifi.it

A. Mariotti · L. Siconolfi · M. V. Salvetti
Dip. Ingegneria Civile e Industriale, Università di Pisa,
Via G. Caruso 8, Pisa 56122, Italia
e-mail: alessandro.mariotti@for.unipi.it

L. Siconolfi
e-mail: siconolfi.lorenzo@gmail.com

M. V. Salvetti
e-mail: mv.salvetti@ing.unipi.it

© Springer Nature Switzerland AG 2019

M. V. Salvetti et al. (eds.), *Direct and Large-Eddy Simulation XI*,
ERCOFTAC Series 25, https://doi.org/10.1007/978-3-030-04915-7_56

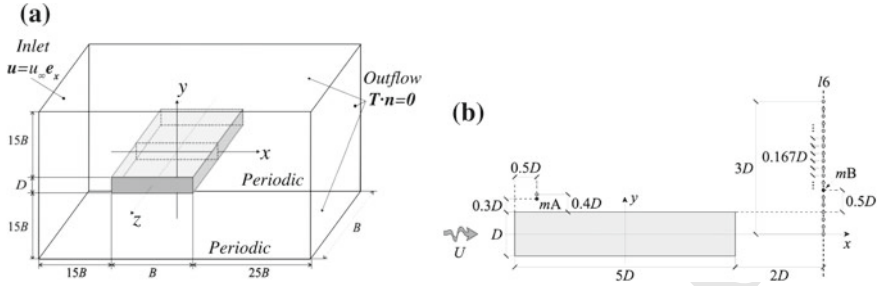


Fig. 1 **a** Sketch of the computational domain; **b** position of anemometry measurement points in the wake of the cylinder ($l6$, mA and mB represent respectively a reference transverse line and two reference points of the benchmark study)

17 contributors were not conclusive to explain the observed dispersion; rather, in some
 18 cases, they led to controversial results. In particular, in a single large-eddy simulation
 19 (LES) contribution [3] a strong sensitivity to the grid resolution in the spanwise direc-
 20 tion was pointed out, but the results obtained for the finest grid significantly deviated
 21 from the ensemble average of those of the experimental and numerical contributions
 22 [2].

23 Recently, a set of LES was carried out in the framework of a stochastic analy-
 24 sis of the sensitivity to grid resolution in the spanwise direction and to the amount
 25 of subgrid scale (SGS) dissipation [4], and further wind tunnel measurements were
 26 obtained for different angles of attack and different oncoming flow turbulence fea-
 27 tures (intensity and integral length scale) [5], including unsteady surface pressures,
 28 forces and wake flow velocities. Experimental data on the flow velocity in the wake
 29 were still completely missing among the BARC contributions.

30 The aim of the present work is to exploit the new sets of LES and experimen-
 31 tal results to give a contribution to highlight the reasons of the dispersion of data
 32 evidenced in the synopsis in [2].

33 2 Simulation and Experiment Set Up

34 LES simulations are carried out for the incompressible flow around a fixed sharp-
 35 edged rectangular cylinder with a chord-to-depth ratio, B/D , equal to 5. The angle of
 36 attack is zero. The computational domain is sketched in Fig. 1a. A uniform velocity
 37 profile is imposed at the inflow (no turbulence), while no-slip conditions are applied
 38 at the solid walls. Periodic conditions are imposed in the spanwise direction, and
 39 traction-free boundary conditions are used at the outflow, on the remaining lateral
 40 sides of the computational domain. Finally, the Reynolds number based on the free-
 41 stream velocity and on the cylinder depth, Re , is equal to 40,000. The sensitivity to
 42 the value of Re was observed to be low [2], although not null [5].

The simulations are performed through an open-source code, Nek5000, based on a high-order accurate spectral-element method (<http://nek5000.mcs.anl.gov>). The order of the Legendre polynomials used as basis functions inside each element is kept herein constant $N = 6$. The grid resolution in the streamwise and lateral directions is $\Delta x = \Delta y = 0.125D$. As for the LES formulation, a simple approach based on the application of a low-pass explicit filter in the modal space, which is characterized by a cut-off k_c , here equal to $N - 3$, and by a weight w , is adopted (see [4] for more details). This modal filter provides a dissipation in the resolved modes that are higher than the cut-off value, and can be interpreted as a SGS dissipation.

The parameters chosen for the sensitivity analysis are the grid resolution in the spanwise direction, defined in terms of the average element size, Δz (in the range $[0.321D, 0.674D]$), and the weight of the explicit filter, w (in the range $[0.01, 0.131]$). The latter has been chosen because it directly controls the amount of SGS dissipation, while the grid resolution in the spanwise direction is investigated because of the high impact of this parameter shown in the LES simulations in [3]. A total of 16 LES simulations were carried out (see [4] for more details).

The wind tunnel tests were conducted in the CRIACIV laboratory at the University of Florence on an aluminum sectional model with a cross section 300×60 mm and a spanwise length of 2.38 m. The model presented very sharp edges, smooth surfaces and high degree of symmetry. For a null angle of attack, the blockage ratio was 3.75%. Unsteady pressure measurements were performed through 61 taps distributed along the midspan section. A single-component hot-wire anemometer allowed the measurement of the fluctuating flow velocities in the wake downstream of the model and in the shear-layer region. The experiments were carried out for Reynolds numbers in the range 12,000 to 110,000, for various angles of attack (up to 10°), in smooth and various grid-induced free-stream turbulent flows (for further details, see [5]).

3 Results and Discussion

Figure 2 shows the distribution over the cylinder side of the pressure coefficient averaged in time, in the spanwise direction and between the upper and lower half perimeters of the cylinder, denoted as $t\text{-avg}(C_p)$, obtained in the 16 LES simulations. As in [2], the local abscissa s/D denotes the distance from the cylinder stagnation point measured along the cylinder side. The considered values of the spanwise spacing of the grid nodes are denoted in the following as Δz_1 to Δz_4 (from the coarsest to the finest), whereas the values of the weight of the explicit filter are indicated as w_1 to w_4 (from the lowest to the highest level of SGS dissipation). It can be seen that most of the calculated C_p distribution are characterized by a recovery occurring upstream compared to the experimental data. As explained in [2], the mean pressure distribution on the body surface is directly related to the curvature of the time-averaged flow streamlines and, in particular, to the shape and length of the main recirculation region on the cylinder sides. Therefore, most parameter combinations lead to a main recirculation region that is significantly shorter than those obtained in most of the BARC contributions. This is consistent with the findings of the most refined LES in

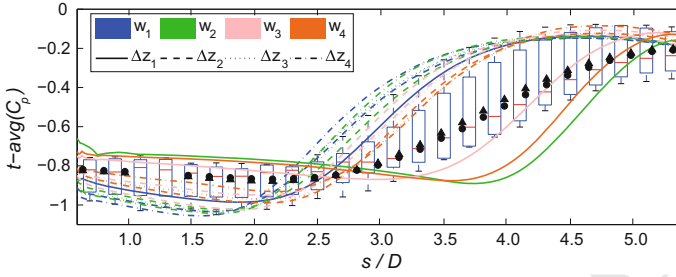


Fig. 2 Mean pressure coefficient on the lateral sides of the prism cross section obtained in the LES analysis. A comparison is provided with the ensemble statistics of the BARC experiments [2] and the experimental data in [5] (circles and triangles refer respectively to $Re = 56,700$ and $112,200$

[3]. In particular, increasing the spanwise resolution and decreasing the SGS dissipation, very small vortical structures, which originate from the instability of the shear layers detaching from the upstream corners, are observed in LES (see [4]), and this behavior corresponds to short main recirculation regions. A similar result was also obtained through detached-eddy simulation (DES) in [6] when reducing the artificial viscosity introduced to stabilize the central-difference scheme for the discretization of the convective term in the governing equations. It is worth noting that a grid with a fine spanwise resolution ($\Delta z = 0.078D$) was employed in that case.

The still open question is whether these perturbations have a physical or a numerical origin. Indeed, the mean C_p distribution obtained in the experiments, reported in Fig. 2, shows that, for low turbulence in the oncoming flow, the length of the plateau, and thus that of the main recirculation region, is significantly longer than that obtained in most of the LES computations, which are yet carried out for smooth oncoming flow. Indeed, the level of flow perturbation upstream of the leading edge separation is negligible in all the LES simulations.

In order to investigate how the differences between experiments and simulations are related to the features and dynamics of the separated shear layers and of the downstream wake, a comparison with the flow velocity measurements reported in [5] is carried out.

Figure 3a shows the mean streamwise velocity profile in the shear-layer region at the point mA of Fig. 1b ($x/D = -2$). The mean velocity profile in the calculations exhibits low uncertainty and a very good agreement with the experiments. In contrast, the standard deviation in time of the velocity fluctuations is very different from one simulation to another, and the experimental data fall inside the uncertainty band (Fig. 3b). Nevertheless, a low level of fluctuations at this streamwise position is not necessarily associated with a long recirculation bubble. Indeed, there are solutions characterized by fluctuations in the shear layer significantly lower than or of the same order as in the experiments that correspond to much shorter mean recirculation regions, as demonstrated by the streamlines in Fig. 4b, d. For example, the simulation with w_1 , Δz_1 , in spite of the very good agreement with the experimental data in terms of flow velocity fluctuations, is characterized by a short bubble. The simula-

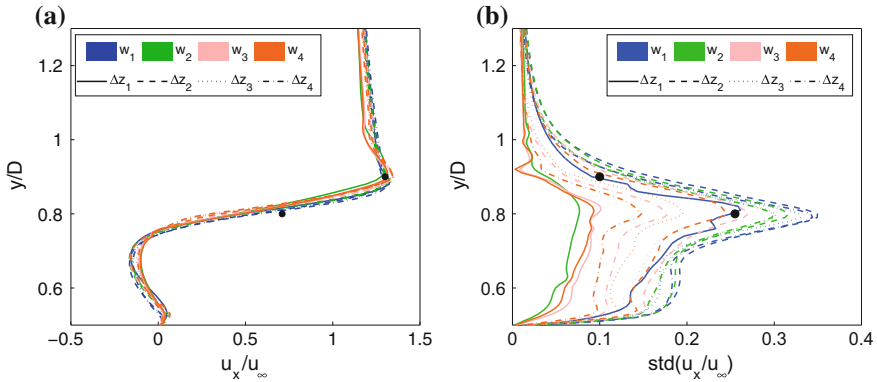


Fig. 3 **a** Mean streamwise velocity profile, and **b** standard deviation of the velocity fluctuations in the x -direction at $x/D = -2$ (see Fig. 1b). The experimental data (black circles) correspond to $Re = 11,800$ [5]

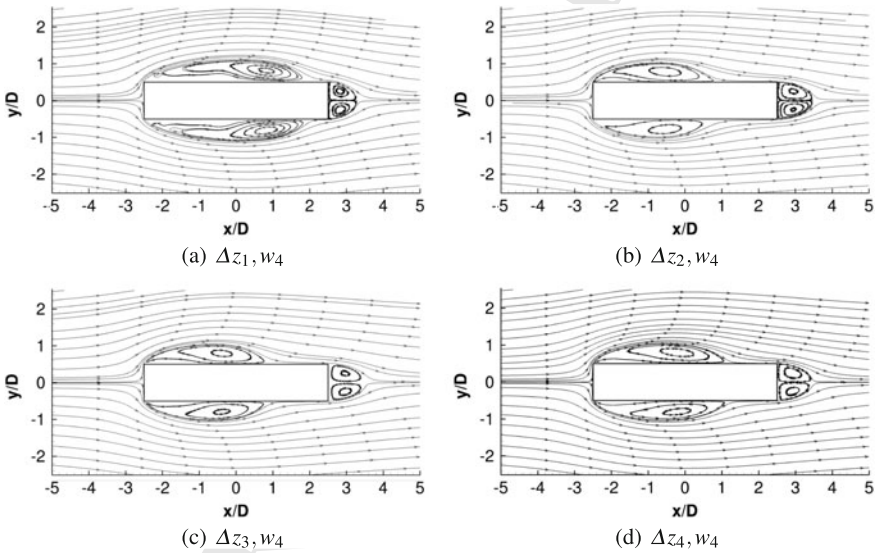


Fig. 4 Mean flow streamlines obtained with LES simulations for four values of the grid spanwise resolution and the same SGS-like dissipation

116 tions with w_4 , Δz_1 and w_4 , Δz_4 have a similar level of fluctuations in the shear layer
 117 being, nonetheless, characterized by significantly different lengths of the recirculation
 118 regions (compare Fig. 4a, d). It is also noteworthy that the behavior of velocity
 119 fluctuations in the bubble and shear layer with the mesh resolution is not monotonous
 120 (see for instance the results for w_4 in Fig. 3b). In conclusion, the comparison with
 121 the available wake measurement data is not yet conclusive, and further analyses are
 122 required in the shear layers at more upstream and downstream locations.

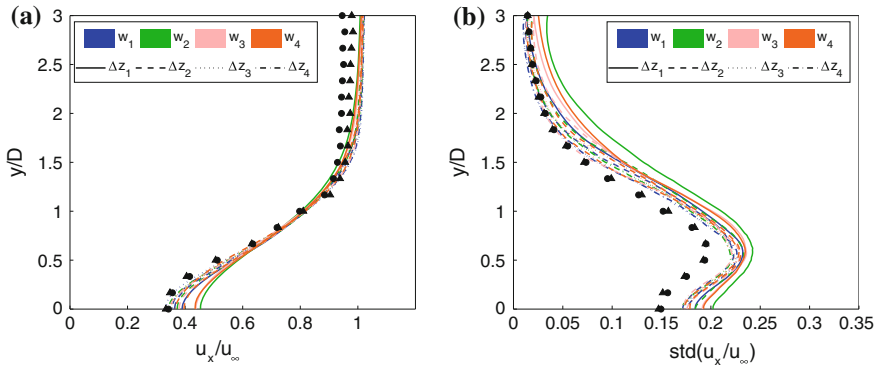


Fig. 5 **a** Mean and **b** standard deviation of the velocity fluctuations in the streamwise x -direction at $x/D = 4.5$ (along line $l6$ in Fig. 1b). Circles and triangles denote the experimental data [5] and refer respectively to $Re = 44,900$ and $112,600$

123 Focusing now on the near wake, Fig. 5 shows the mean velocity profile and the
 124 standard deviation of the velocity fluctuations in the streamwise direction along
 125 the line $l6$ of Fig. 1b. It is clear that, in spite of the large differences observed in
 126 the flow on the cylinder lateral surface, the dispersion of the results in the wake is small
 127 and the agreement with the hot-wire anemometry measurements is good, especially
 128 for the mean velocity profile. Such a result suggests that the interaction between the
 129 wake behind the cylinder and the upstream dynamics near the body is rather weak,
 130 and that the mesh resolution and artificial dissipation have a minor influence on the
 131 former.

132 References

- 133 1. Nakamura, Y., Ohya, Y., Tsuruta, H.: Experiments on vortex shedding from flat plates with
 134 square leading and trailing edges. *J. Fluid Mech.* **222**, 437–447 (1991)
- 135 2. Bruno, L., Salvetti, M.V., Ricciardelli, F.: Benchmark on the aerodynamics of a rectangular 5:1
 136 cylinder: an overview after the first four years of activity. *J. Wind Eng. Ind. Aerodyn.* **126**,
 137 87–106 (2014)
- 138 3. Bruno, L., Coste, N., Fransos, D.: Simulated flow around a rectangular 5:1 cylinder: spanwise
 139 discretisation effects and emerging flow features. *J. Wind Eng. Ind. Aerodyn.* **104–106**, 203–215
 140 (2012)
- 141 4. Mariotti, A., Siconolfi, L., Salvetti, M.V.: Stochastic sensitivity analysis of large-eddy simulation
 142 predictions of the flow around a 5:1 rectangular cylinder. *Eur. J. Mech. B-Fluid* **62**, 149–165
 143 (2017)
- 144 5. Mannini, C., Marra, A.M., Pigolotti, L., Bartoli, G.: The effects of free-stream turbulence and
 145 angle of attack on the aerodynamics of a cylinder with rectangular 5:1 cross section. *J. Wind
 146 Eng. Ind. Aerodyn.* **161**, 42–58 (2017)
- 147 6. Mannini, C., Soda, S., Schewe, G.: Numerical investigation on the three-dimensional unsteady
 148 flow past a 5:1 rectangular cylinder. *J. Wind Eng. Ind. Aerodyn.* **99**, 469–482 (2011)

MARKED PROOF

Please correct and return this set

Please use the proof correction marks shown below for all alterations and corrections. If you wish to return your proof by fax you should ensure that all amendments are written clearly in dark ink and are made well within the page margins.

<i>Instruction to printer</i>	<i>Textual mark</i>	<i>Marginal mark</i>
Leave unchanged	... under matter to remain	Ⓟ
Insert in text the matter indicated in the margin	∧	New matter followed by ∧ or ∧ [Ⓢ]
Delete	/ through single character, rule or underline or ┌───┐ through all characters to be deleted	Ⓞ or Ⓞ [Ⓢ]
Substitute character or substitute part of one or more word(s)	/ through letter or ┌───┐ through characters	new character / or new characters /
Change to italics	— under matter to be changed	↵
Change to capitals	≡ under matter to be changed	≡
Change to small capitals	≡ under matter to be changed	≡
Change to bold type	~ under matter to be changed	~
Change to bold italic	⌘ under matter to be changed	⌘
Change to lower case	Encircle matter to be changed	⊖
Change italic to upright type	(As above)	⊕
Change bold to non-bold type	(As above)	⊖
Insert 'superior' character	/ through character or ∧ where required	Υ or Υ under character e.g. Υ or Υ
Insert 'inferior' character	(As above)	∧ over character e.g. ∧
Insert full stop	(As above)	⊙
Insert comma	(As above)	,
Insert single quotation marks	(As above)	ʹ or ʸ and/or ʹ or ʸ
Insert double quotation marks	(As above)	“ or ” and/or ” or ”
Insert hyphen	(As above)	⊖
Start new paragraph	┌	┌
No new paragraph	┐	┐
Transpose	└┐	└┐
Close up	linking ○ characters	Ⓞ
Insert or substitute space between characters or words	/ through character or ∧ where required	Υ
Reduce space between characters or words		↑